

A Study of the Polarities, Anisotropic Polarisabilities and Carbonyl Infrared Vibrational Frequencies of the Complexes $[M(CO)_5\{P(OCH_2)_3CMe\}]$ ($M = Cr, Mo$ or W) and the Crystal Structure of $[Mo(CO)_5\{P(OCH_2)_3CMe\}]$: Evidence for π -Acceptor Behaviour in Co-ordinated Phosphorus†

Manuel J. Aroney,* Murray S. Davies, Trevor W. Hambley and Raymond K. Pierens
Department of Inorganic Chemistry, The University of Sydney, Sydney, NSW 2006, Australia

Studies of electric dipole moments, electric birefringences, carbonyl infrared frequencies and interatomic bond distances provide mutually reinforcing evidence for π -acid behaviour of the bicyclic phosphite ligand in $[M(CO)_5\{P(OCH_2)_3CMe\}]$ complexes ($M = Cr, Mo$ or W). Molecular optical anisotropies and directional polarisabilities from experiment are analysed to show strong polarisability enhancement along the molecular symmetry axis and concomitant diminution of polarisability perpendicular to that axis, relative to a hypothetical σ -bonded P–M model. The results provide evidence for a highly deformable π -component in the phosphorus–metal bonding and for a π -delocalised P–M–CO(*trans*) system. Comparisons are made with other $[M(CO)_5L]$ compounds where $L =$ quinuclidine, PMe_3 or PCl_3 . The crystal structure of $[Mo(CO)_5\{P(OCH_2)_3CMe\}]$ is reported and bond dimensions are compared with those of related molybdenum complexes.

Much effort has been devoted to investigating metal–phosphorus bonding in complexes of transition-metals with tertiary phosphine or phosphite ligands.^{1–9} Arguments have been advanced both for and against π -acid behaviour of PZ_3 (where $Z =$ alkyl, aryl, halogen, methoxy, *etc.*) in addition to their role as σ donors. The most recent published works generally contend that π -acceptor behaviour is important for PZ_3 ligands particularly if the substituents Z are strongly electron withdrawing.⁹

The issue of π back-bonding has remained controversial because the interpretation of physical evidence is often complicated by the postulated synergism between the σ - and π -bonding mechanisms in the metal–phosphorus (M–P) bond. The conventional picture is that of π -electron transfer from filled metal d orbitals to empty phosphorus 3d orbitals; the π bonding is enhanced by highly electronegative Z substituents which would contract the phosphorus 3d orbitals and lower their energy.¹ Other models of π acceptance by PZ_3 derived from quantum mechanical calculations, involve P–Z σ^* acceptor orbitals^{10,11} or combination of these with 3d orbitals of phosphorus.⁹

The present work is part of a continuing programme of study of metal–ligand interactions in complexes of the form $[M(CO)_5L]$.^{12–14} Electric dipole moments, electric birefringences and infrared carbonyl stretching frequencies are reported for $[M(CO)_5L]$ complexes ($M = Cr, Mo$ or W ; $L =$ 4-methyl-1-phospha-2,6,7-trioxabicyclo[2.2.2]octane) and these are compared with data for the analogous compounds where $L =$ quinuclidine (qncd), PMe_3 or PCl_3 . The bicyclic phosphite ligand, like quinuclidine, has a relatively rigid structure in which the alkyl constituents of the ligands are constrained to minimise steric buttressing of the equatorial carbonyls and to eliminate the possibility of ligand conformational change on complexation; the importance of such steric interactions has been extensively examined by Brown and co-workers.^{15–17} In addition, these ligands have a high degree of

symmetry which facilitates interpretation of the present experimental data. An X-ray crystal structure determination of $[Mo(CO)_5\{P(OCH_2)_3CMe\}]$ is also presented.

Experimental

Syntheses.—The phosphite $P(OCH_2)_3CMe$ was prepared by a modification of the method of Verkade and co-workers^{18,19} by stirring 1,1,1-tris(hydroxymethyl)ethane and triethylphosphite under nitrogen for 7 d followed by refluxing for 3 h to ensure completion of reaction. The solvent was removed *in vacuo* and the residue recrystallised from hexane. The product was characterised by comparison of its melting point and proton NMR spectrum with literature.^{18–21}

The $[M(CO)_5\{P(OCH_2)_3CMe\}]$ ($M = Cr, Mo$ or W) complexes were prepared according to the method of Verkade *et al.*²⁰ Compound purities were determined by melting point and carbonyl infrared spectral comparison with the reported values.

Dipole Moment and Electro-optical Kerr Effect.—Solute electric dipole moments μ and electric birefringences, the latter expressed as molar Kerr constants ${}_mK$, were determined in 1,4-dioxane at 298K and for sodium D-light (589 nm). Solubility limitations precluded the use of cyclohexane or CCl_4 as solvents. The experimental procedures, symbols and treatment of data are described in refs. 22 and 23.

Infrared Spectra.—These were recorded on a Digilab FTS 20/80 Fourier-transform infrared spectrometer for tetrahydrofuran solutions with solute concentrations of 2–4 mmol dm⁻³.

X-Ray Crystal Structure Analysis.—Crystals of $[Mo(CO)_5\{P(OCH_2)_3CMe\}]$ suitable for X-ray analysis were grown by vapour diffusion from tetrahydrofuran–pentane. For structural analysis a crystal was mounted on a glass fibre with cyanocrylate resin.

Crystal data. $C_{10}H_9MoO_8P$, $M = 384.09$, monoclinic, $a = 10.616(2)$, $b = 10.787(5)$, $c = 12.459(3)$ Å, $\beta = 98.03(2)^\circ$, $U = 1412.8$ Å³ (by least-squares refinement to the setting

† Supplementary data available: see Instructions for Authors, *J. Chem. Soc., Dalton Trans.*, 1994, Issue 1, pp. xxiii–xxviii.

parameters of 25 independent reflections), space group $P2_1/c$, $Z = 4$, $D_c = 1.806 \text{ g cm}^{-3}$, $F(000) = 760$. Colourless, air stable crystals. Crystal dimensions $0.38 \times 0.12 \times 0.02 \text{ mm}$, $\mu(\text{Mo-K}\alpha) = 10.09 \text{ cm}^{-1}$, $\lambda(\text{Mo-K}\alpha) = 0.7107 \text{ \AA}$.

Data collection and processing. CAD4F diffractometer, (ω -0.330) mode with scan width $1.10 + 0.34 \tan\theta$, graphite-monochromated Mo-K α radiation; 2199 reflections collected ($1 < \theta < 23^\circ$, $\pm h, k, l$), 1257 with $I > 2.5\sigma(I)$ were considered observed [merging $R = 0.030$ after absorption correction (max., min. transmission factors = 0.853, 0.774)].²⁴ No decomposition was observed during collection.

Structure analysis and refinement. Heavy-atom methods using SHELX 76²⁵ and the solution was extended by Fourier-difference methods. Full-matrix least-squares refinement with all non-hydrogen atoms anisotropic and hydrogens in calculated positions with isotropic thermal parameters. The weighting scheme was $w = 1.003/[\sigma^2(F_o) + 0.00041F_o^2]$ with $R [= \Sigma(|F_o| - |F_c|)/\Sigma|F_o|]$ and $R' [= \Sigma w(|F_o| - |F_c|)^2/\Sigma wF_o^2]^\ddagger$ values of 0.030 and 0.032. Maximum excursions in a final difference map were $+0.3 \text{ e \AA}^{-3}$ and -0.4 e \AA^{-3} . Scattering factors and anomalous dispersion terms for Mo were taken from ref. 26 and all others used were those supplied in SHELX 76. All calculations were carried out using SHELX 76 and plots drawn using ORTEP.²⁷

Additional material available from the Cambridge Crystallographic Data Centre comprises H-atom coordinates, thermal parameters and remaining bond lengths and angles.

Results and Discussion

Infrared Spectra.—For each complex $[\text{M}(\text{CO})_5\text{L}]$ in tetrahydrofuran, two A_1 , E and B_1 vibrational modes (the latter formally infrared forbidden) are observed.^{28,29} Retaining the same ligand L, only small variations are found with change of metal. From the data in Table 1, the carbonyl stretching frequencies of the $[\text{M}(\text{CO})_5\{\text{P}(\text{OCH}_2)_3\text{CMe}\}]$ complexes are seen to be intermediate between those of the corresponding PMe_3 and PCl_3 complexes. The A_{1ax} absorption appears the most responsive to change in the ligand L. Trends in $\nu(\text{CO})$, and especially for A_{1ax} , suggest that the ligands L have electron withdrawing capacity in the order $\text{qncd} < \text{PMe}_3 < \text{P}(\text{OCH}_2)_3\text{CMe} < \text{PCl}_3$, with $\text{P}(\text{OCH}_2)_3\text{CMe}$ relatively close to PMe_3 . They suggest also that this is the order of increasing π character for the connecting L–M bond in the complexes, a result in accord with the π -acceptor sequence on p. 436 of ref. 2.

Electric Dipole Moments.—The experimental μ values are listed in column 2 of Table 2. Verkade²¹ has shown that the moment vector of $\text{P}(\text{OCH}_2)_3\text{CMe}$ is directed along the molecular three-fold symmetry axis with the negative pole in proximity to the P atom. He comments that the oxygens of this ligand have appreciable sp^2 character which 'favours drift of electron density from the unhybridised filled p orbital on each oxygen into available d orbitals on phosphorus'. This correlates with values of ca. 115° for the P–O–C bond angles of this ligand, see pp. 13, 14 of ref. 21 and the crystal structure of $[\text{Mo}(\text{CO})_5\{\text{P}(\text{OCH}_2)_3\text{CMe}\}]$ described below.

The complexes $[\text{M}(\text{CO})_5\{\text{P}(\text{OCH}_2)_3\text{CMe}\}]$ are highly dipolar having μ values of the order 23–25 ($\times 10^{-30} \text{ Cm}$). Molecular moments calculated from simple vector additivity as $\mu[\text{M}(\text{CO})_5(\text{qncd})] - \mu(\text{qncd}) + \mu[\text{P}(\text{OCH}_2)_3\text{CMe}]$ are 29.8, 31.0 and $31.5 (\times 10^{-30} \text{ C m})$ respectively for $\text{M} = \text{Cr, Mo}$ and W ; * *i.e.* they are substantially greater than the moments from experiment for the $[\text{M}(\text{CO})_5\{\text{P}(\text{OCH}_2)_3\text{CMe}\}]$ complexes. It is unlikely that disparity of this magnitude would be due solely to differences in the σ -donor ability of phosphorus relative to

Table 1 Infrared carbonyl stretching frequencies (cm^{-1}) for solutes in tetrahydrofuran^{a,b}

Solute	A_{1eq}^c	B_1	A_{1ax}^c	E
$[\text{Cr}(\text{CO})_5\{\text{P}(\text{OCH}_2)_3\text{CMe}\}]$	2077	1994	1955	1955
$[\text{Mo}(\text{CO})_5\{\text{P}(\text{OCH}_2)_3\text{CMe}\}]$	2083	1998	1959	1959
$[\text{W}(\text{CO})_5\{\text{P}(\text{OCH}_2)_3\text{CMe}\}]$	2083	1989	1952	1952
$[\text{Cr}(\text{CO})_5(\text{PMe}_3)]$	2061	1976	1943	1934
$[\text{W}(\text{CO})_5(\text{PMe}_3)]$	2069	1976	1942	1932
$[\text{Cr}(\text{CO})_5(\text{PCl}_3)]$	2089	2018	2002	1978
$[\text{W}(\text{CO})_5(\text{PCl}_3)]$	2095	2017	1996	1974
$[\text{Cr}(\text{CO})_5(\text{qncd})]$	2063	1964	1894	1929
$[\text{W}(\text{CO})_5(\text{qncd})]$	2066	1963	1888	1921

^a Uncertainty in ν is $\pm 0.5 \text{ cm}^{-1}$. ^b Carbonyl frequencies for the PMe_3 , PCl_3 and qncd complexes are in general agreement with earlier values in alkane solution^{13,14} apart from $\nu(\text{CO})_{A_{1ax}}$ for the quinuclidine complexes which are 21–28 cm^{-1} lower in tetrahydrofuran. ^c A_{1eq} and A_{1ax} refer, in turn, to the equatorial and axial symmetric CO stretches.

nitrogen in the ligands. Support for this comes from the closeness of the dipole moments of NMe_3BH_3 and PMe_3BH_3 which are respectively 16.1 ± 0.3 and $16.6 \pm 0.7 (\times 10^{-30} \text{ C m})$ as determined by Kuczkowski and co-workers^{31,32} from Stark splitting of the microwave spectra for these compounds.

In the case of $[\text{M}(\text{CO})_5(\text{PMe}_3)]$ complexes, dipole moments calculated as $\mu[\text{M}(\text{CO})_5(\text{qncd})] - \mu(\text{qncd}) + \mu(\text{PMe}_3)^\ddagger$ are 20.0, 21.2 and $21.7 (\times 10^{-30} \text{ C m})$ for $\text{M} = \text{Cr, Mo}$ and W , respectively, and these also exceed the experimental values which are, in turn, 16.9, 17.3 and $17.7 (\times 10^{-30} \text{ C m})$.¹⁴

Similar calculations for complexes $[\text{M}(\text{CO})_5(\text{PCl}_3)]$, using $\mu(\text{PCl}_3)$ in place of $\mu(\text{PMe}_3)$ in the above relation, lead to 13.0 and $14.7 (\times 10^{-30} \text{ C m})$ for $[\text{Cr}(\text{CO})_5(\text{PCl}_3)]$ and $[\text{W}(\text{CO})_5(\text{PCl}_3)]$, respectively, *i.e.* the $\mu(\text{calc.})$ values are much greater than the measured moments both of which are $2.80 \times 10^{-30} \text{ C m}$.¹⁴

The differences $\Delta\mu = \mu(\text{calc.}) - \mu(\text{expl.})$ for the $[\text{M}(\text{CO})_5\text{L}]$ complexes are 3.1–4.0 ($\text{L} = \text{PMe}_3$), 6.3–6.8 [$\text{L} = \text{P}(\text{OCH}_2)_3\text{CMe}$] and 10.2–11.9 ($\text{L} = \text{PCl}_3$) (all $\times 10^{-30} \text{ C m}$). These can be rationalised to indicate decreasing $\text{L} \rightarrow \text{M}$ σ donation and/or increasing $\text{L} \leftarrow \text{M}$ π -acceptor behaviour for the ligand sequence qncd , PMe_3 , $\text{P}(\text{OCH}_2)_3\text{CMe}$ and PCl_3 , and as such they correlate with the results from the infrared data. As intuitively expected, the $\Delta\mu$ values are greatest with the bicyclic phosphite and PCl_3 ligands because of the electron-withdrawing properties of the O and Cl atoms. It is not possible, however, to separate the σ - and π -electronic factors in the metal–ligand bonding and to gauge their relative importance from dipole moment analysis alone.

Molecular Polarisabilities.—The measured molar Kerr constants in column 3 of Table 2 translate into the molecular polarisability anisotropies Γ of column 4, by way of the Le Fèvre modified Langevin-Born equation (1).³⁴

$${}_mK = (N/405kT\epsilon_0)[(\text{D}P/\epsilon P)\Gamma^2 + (kT)^{-1}\mu^2\Gamma] \quad (1)$$

In this work Γ is defined as $(b_1 - b_2)$ where b_1 is the molecular electron polarisability in the direction of the molecular dipole vector, *i.e.* along the phosphorus–metal bond

[†] The dipole moment of PMe_3 is $3.97 \times 10^{-30} \text{ C m}$.³³ The assumption is made in the calculations that the dipole vector for this molecule has the negative pole in proximity to the phosphorus. If the sense of the PMe_3 dipole vector were reversed, then the predicted moments for $[\text{M}(\text{CO})_5(\text{PMe}_3)]$ would be 12.0, 13.2 and $13.7 (\times 10^{-30} \text{ C m})$ respectively. These values, however, appear less likely since they lead to the conclusion that the experimental moments of $[\text{M}(\text{CO})_5(\text{PMe}_3)]$ are even larger than those of the σ -bonded P–M model for these complexes.

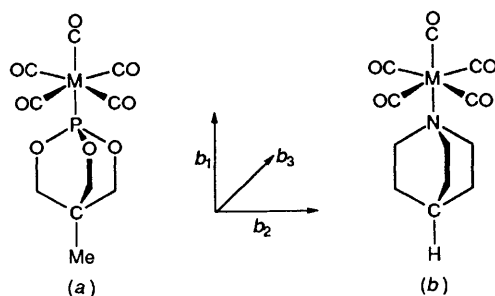
[‡] The dipole moment of PCl_3 is $3.04 \times 10^{-30} \text{ C m}$.¹⁴ The experimental moment of $[\text{Mo}(\text{CO})_5(\text{PCl}_3)]$ has not been reported.

* Measured μ for qncd and for $[\text{M}(\text{CO})_5(\text{qncd})]$ complexes are 3.8, 19.8, 21.0 and $21.5 (\times 10^{-30} \text{ C m})$;¹³ the last three values are for $\text{M} = \text{Cr, Mo}$ and W , respectively.

Table 2 Electric dipole moments, molar Kerr constants and molecular polarisability anisotropies at infinite dilution in 1,4-dioxane and at 298 K and $\lambda = 589 \text{ nm}^a$

Solute	$\mu^b/10^{-30} \text{ C m}$	${}_mK/10^{-27} \text{ m}^5 \text{ V}^{-2} \text{ mol}^{-1}$	$\Gamma^c/10^{-40} \text{ C m}^2 \text{ V}^{-1}$
$\text{P}(\text{OCH}_2)_3\text{CMe}$	13.8 ^d	409 ^d	2.13 (-426)
$[\text{Cr}(\text{CO})_5\{\text{P}(\text{OCH}_2)_3\text{CMe}\}]$	23.0 ± 0.4	1097 ± 17	$2.08 \pm 0.03 (-1172 \pm 18)$
$[\text{Mo}(\text{CO})_5\{\text{P}(\text{OCH}_2)_3\text{CMe}\}]$	24.3 ± 0.4	1215 ± 28	$2.07 \pm 0.05 (-1309 \pm 30)$
$[\text{W}(\text{CO})_5\{\text{P}(\text{OCH}_2)_3\text{CMe}\}]$	25.2 ± 0.3	1381 ± 43	$2.18 \pm 0.09 (-1411 \pm 56)$

^a Dipole moments, molar Kerr constants and polarisabilities are expressed in SI units. The conversion factors from the electrostatic (cgs, esu) system are, respectively: $1 \text{ C m} = 0.2998 \times 10^{30} \text{ D}$, $1 \text{ m}^5 \text{ V}^{-2} \text{ mol}^{-1} = 0.8988 \times 10^{15} \text{ esu mol}^{-1}$, $1 \text{ C m}^2 \text{ V}^{-1} = 0.8988 \times 10^{16} \text{ cm}^3$. ^b Dipole moments of the complexes were obtained taking the molar distortion polarisation as 1.05 times the molecular D-line refractivity.^{23c} ^c An alternative value from the solution of the quadratic equation in Γ is shown in parentheses. ^d Quoted from ref. 30; errors were not specified.

**Fig. 1** Structure representation of (a) $[\text{M}(\text{CO})_5\{\text{P}(\text{OCH}_2)_3\text{CMe}\}]$ and (b) $[\text{M}(\text{CO})_5(\text{qncd})]$

axis; b_2 and b_3 are the polarisabilities perpendicular to that direction (see Fig. 1). From symmetry, $b_2 = b_3$. The terms N , k , T and ϵ_0 refer in turn to Avogadro's number, the Boltzmann constant, the absolute temperature and the permittivity of a vacuum. The ratios molar distortion polarisation/molar electron polarisation (${}_D P/{}_E P$) were taken as 1.1, a sufficiently good approximation for this work.³⁵

Solution of the quadratic equation (1) yields two possible values of Γ for each molecule and these are shown in column 4 of Table 2. The Γ values in parentheses are not physically meaningful* and are disregarded.

The anisotropies Γ of the three complexes are closely similar to each other and to the free $\text{P}(\text{OCH}_2)_3\text{CMe}$ ligand. For each complex, the molecular polarisability tensor is such that $b_1 > b_2$, i.e. the direction of maximum polarisability is along the P-M bond axis. This is in marked contrast to the analogous $[\text{M}(\text{CO})_5(\text{qncd})]$ complexes for which measured Γ^\dagger values of -4.7 , -4.9 and -5.0 ($\times 10^{-40} \text{ C m}^2 \text{ V}^{-1}$) have been reported ($M = \text{Cr}$, Mo and W , respectively) and for which the N-M bond direction coincides with the axis of minimum molecular polarisability.¹³ Both ${}_mK$ and Γ are sensitively responsive to subtle differences in electronic behaviour between the P-M and the N-M bonded $[\text{M}(\text{CO})_5\text{L}]$ systems.

From segment polarisability additivity,³⁴ the molecular anisotropy $\Gamma(\sigma)$ can be predicted for a hypothetical $[\text{M}(\text{CO})_5\{\text{P}(\text{OCH}_2)_3\text{CMe}\}]$ model in which the P-M bond connecting the $\text{P}(\text{OCH}_2)_3\text{CMe}$ and $\text{M}(\text{CO})_5$ groupings has purely σ character. The procedure essentially is that previously described in ref. 13. To a good approximation, $\Gamma(\sigma)$ for $[\text{M}(\text{CO})_5\{\text{P}(\text{OCH}_2)_3\text{CMe}\}]$ can be obtained as $\Gamma(\text{expl.})[\text{M}(\text{CO})_5(\text{qncd})] - \Gamma(\text{expl.})(\text{qncd}) + \Gamma(\text{expl.})[\text{P}(\text{OCH}_2)_3\text{CMe}]$. For the free qncd molecule $\Gamma(\text{expl.})$ is 0.18 ($\times 10^{-40} \text{ C m}^2 \text{ V}^{-1}$).¹³

* The negative values of Γ in Table 2, used in conjunction with Σb_i for these molecules (from refractivity measurements), lead to the following b_1 and b_2 ($=b_3$): -270 and 156 for $\text{P}(\text{OCH}_2)_3\text{CMe}$; -750 ± 12 and 423 ± 6 for $[\text{Cr}(\text{CO})_5\{\text{P}(\text{OCH}_2)_3\text{CMe}\}]$; -838 ± 21 and 471 ± 11 for $[\text{Mo}(\text{CO})_5\{\text{P}(\text{OCH}_2)_3\text{CMe}\}]$; -904 ± 38 and 507 ± 19 for $[\text{W}(\text{CO})_5\{\text{P}(\text{OCH}_2)_3\text{CMe}\}]$.

† The Γ values given here for the $[\text{M}(\text{CO})_5(\text{qncd})]$ complexes are one half of the molecular anisotropies shown in Table 2 of ref. 13; in that paper Γ was defined as $2b_1 - b_2 - b_3$.

The $\Gamma(\sigma)$ values so calculated are compared with the molecular anisotropies from experiment; $\Gamma(\sigma)$ and $\Gamma(\text{expl.})$ are respectively listed in columns 2 and 3 of Table 3. Differences $\Delta\Gamma$, defined as $\Gamma(\text{expl.}) - \Gamma(\sigma)$, are given in column 4. It is seen that $\Delta\Gamma$ for each $[\text{M}(\text{CO})_5\{\text{P}(\text{OCH}_2)_3\text{CMe}\}]$ complex is large and positive, 5.1 ± 0.2 ($\times 10^{-40} \text{ C m}^2 \text{ V}^{-1}$), an important result in that it clearly illustrates the inadequacy of the P-M σ -bonded model for these complexes. Such $\Delta\Gamma$ values are too great to be explained by possible variations in the anisotropy of $\text{P}(\text{OCH}_2)_3\text{CMe}$ or quinuclidine consequent to co-ordinate bond formation. The tying up of P or N lone pair electrons in a σ bond results in only small changes in anisotropy ($< 1 \times 10^{-40} \text{ C m}^2 \text{ V}^{-1}$) as evidenced from the following experimental determinations of $\Gamma/10^{-40} \text{ C m}^2 \text{ V}^{-1}$: -0.7 (PMe_3),³³ -0.2 (OPMe_3),³³ 2.1 [$\text{P}(\text{OCH}_2)_3\text{CMe}$], 3.0 [$\text{OP}(\text{OCH}_2)_3\text{CMe}$],³⁰ -0.3 (NMe_3),³⁶ 0.5 (ONMe_3),³⁶ 0.1 ($\text{BH}_3\text{-NMe}_3$).³⁷ The reason for the large disparity $\Delta\Gamma$ is primarily to be found in the interaction between the $\text{P}(\text{OCH}_2)_3\text{CMe}$ and $\text{M}(\text{CO})_5$ fragments beyond that of σ -bond formation. This interaction results in an electronic system which, relative to the σ -bond model, has greatly enhanced polarisability along the molecular symmetry axis.

The approach is extended to comparing $\Delta\Gamma$ for the complexes $[\text{M}(\text{CO})_5\{\text{P}(\text{OCH}_2)_3\text{CMe}\}]$, $[\text{M}(\text{CO})_5(\text{PMe}_3)]$ and $[\text{M}(\text{CO})_5(\text{PCl}_3)]$. Predicted values of $\Gamma(\sigma)$ for the latter two groups are obtained as $\Gamma(\text{expl.})[\text{M}(\text{CO})_5(\text{qncd})] - \Gamma(\text{expl.})(\text{qncd}) + \Gamma(\text{expl.})(\text{PMe}_3$ or $\text{PCl}_3)$. The experimental anisotropies of PMe_3 and PCl_3 are respectively -0.73 and -0.87 ($\times 10^{-40} \text{ C m}^2 \text{ V}^{-1}$).^{14,33} The following $\Delta\Gamma/10^{-40} \text{ C m}^2 \text{ V}^{-1}$ are found: 5.1 – 5.4 for $[\text{M}(\text{CO})_5(\text{PMe}_3)]$, 4.9 – 5.3 for $[\text{M}(\text{CO})_5\{\text{P}(\text{OCH}_2)_3\text{CMe}\}]$ and 7.5 – 7.6 for $[\text{M}(\text{CO})_5(\text{PCl}_3)]$. The estimated uncertainty in $\Delta\Gamma$ is $\pm 0.4 \times 10^{-40} \text{ C m}^2 \text{ V}^{-1}$ so that it is not possible to differentiate between the PMe_3 and the $\text{P}(\text{OCH}_2)_3\text{CMe}$ complexes on the basis of this property. Polarisability exaltation along P-M-CO(*trans*) is greatest for $[\text{M}(\text{CO})_5(\text{PCl}_3)]$ providing independent confirmation for a more deformable π system in the PCl_3 complexes.

Further analysis of the data involves the derivation of the principal polarisabilities $b_i(\text{expl.})$ which are shown in column 5 of Table 3. These follow from $\Gamma(\text{expl.})$ and the sum Σb_i obtained from refractivity data using equation (2).³⁴

$${}_E P = N(b_1 + 2b_2)/9\epsilon_0 \quad (2)$$

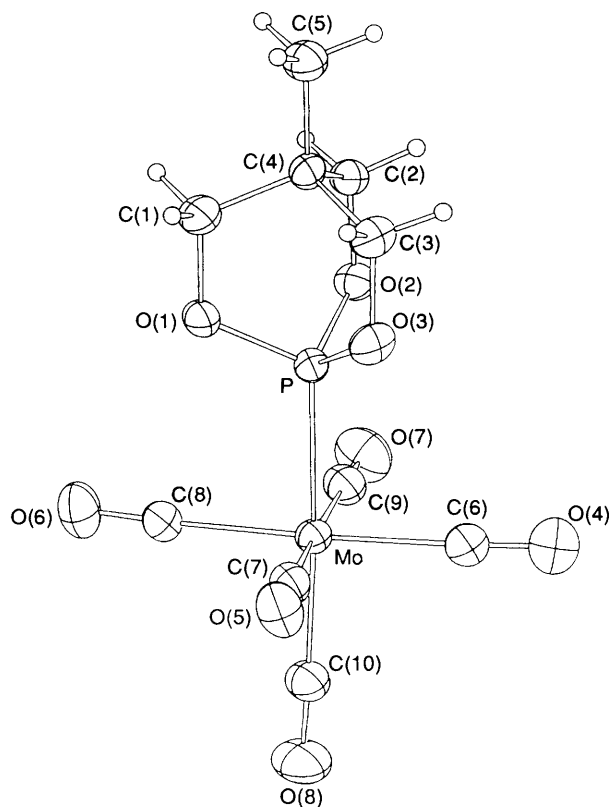
The molar electron polarisation was taken as 0.95 times the molecular refractivity for $\lambda = 589 \text{ nm}$. The experimental R_D values are 33.1 cm^3 for $\text{P}(\text{OCH}_2)_3\text{CMe}$; 76.7 , 83.0 and 87.4 cm^3 for $[\text{M}(\text{CO})_5\{\text{P}(\text{OCH}_2)_3\text{CMe}\}]$ where M is Cr, Mo and W, respectively. The $b_i(\sigma)$ values in column 6 were calculated as $b_i(\text{expl.})[\text{M}(\text{CO})_5(\text{qncd})] - b_i(\text{expl.})(\text{qncd}) + b_i[\text{P}(\text{OCH}_2)_3\text{CMe}]$.[‡] Differences $\Delta b_i = b_i(\text{expl.}) - b_i(\sigma)$ are listed in column 7.

‡ The following $b_i(\text{expl.})$ and $b_2(\text{expl.})$ values/ $10^{-40} \text{ C m}^2 \text{ V}^{-1}$ were used: 14.4 , 14.2 (qncd); 30.3 , 35.1 [$\text{Cr}(\text{CO})_5(\text{qncd})$]; 32.8 , 37.8 [$\text{Mo}(\text{CO})_5(\text{qncd})$]; 33.1 , 38.1 [$\text{W}(\text{CO})_5(\text{qncd})$] (all from ref. 13); 15.3 , 13.2 [$\text{P}(\text{OCH}_2)_3\text{CMe}$] (present work).

Table 3 Comparison of the experimental polarisability anisotropies ($\Gamma/10^{-40}\text{C m}^2\text{ V}^{-1}$) and principal polarisabilities ($b_i^*/10^{-40}\text{C m}^2\text{ V}^{-1}$) of $[\text{M}(\text{CO})_5\{\text{P}(\text{OCH}_2)_3\text{CMe}\}]$ complexes with values calculated for a σ -bonded P-M model

Complex	$\Gamma(\sigma)$	$\Gamma(\text{expl.})$	$\Delta\Gamma$	$b_i(\text{expl.})$	$b_i(\sigma)$	Δb_i
$[\text{Cr}(\text{CO})_5\{\text{P}(\text{OCH}_2)_3\text{CMe}\}]$	-2.8	2.08	4.9	$b_1 = 33.4$ $b_2 = 31.4$	31.2 34.1	2.2 -2.7
$[\text{Mo}(\text{CO})_5\{\text{P}(\text{OCH}_2)_3\text{CMe}\}]$	-3.0	2.07	5.1	$b_1 = 36.1$ $b_2 = 34.1$	33.7 36.8	2.4 -2.7
$[\text{W}(\text{CO})_5\{\text{P}(\text{OCH}_2)_3\text{CMe}\}]$	-3.1	2.18	5.3	$b_1 = 38.1$ $b_2 = 35.9$	34.0 37.1	4.1 -1.2

* Uncertainty in $b_i(\text{expl.})$ values is ± 0.3 , ± 0.5 and ± 0.6 ($\times 10^{-40}\text{C m}^2\text{ V}^{-1}$) for the Cr, Mo and W complex, respectively.

**Fig. 2** ORTEP²⁷ plot (30% thermal ellipsoids) with atomic numbering of $[\text{Mo}(\text{CO})_5\{\text{P}(\text{OCH}_2)_3\text{CMe}\}]$

For each complex $b_1(\text{expl.})$ is substantially greater than the calculated value for the σ model (Δb_1 positive) while the molecular transverse polarisabilities $b_2(\text{expl.})$ and $b_3(\text{expl.})$ are smaller than the calculated values (Δb_2 , Δb_3 negative). Estimated uncertainties in Δb_i are ± 0.6 , ± 0.8 and ± 0.9 ($\times 10^{-40}\text{C m}^2\text{ V}^{-1}$), respectively, for the Cr, Mo and W complexes.

Le Fèvre³⁴ has found that π electrons are much more polarisable than the more tightly bound σ electrons and that this is especially so along the bond axis. It has also been shown^{34,38-40} that in delocalised electron systems, polarisability enhancement above that predicted from the valence optical scheme of group additivity, occurs in the direction of maximum electromeric shift and a decrease of polarisability is found perpendicular to that direction.

The present results classically conform to the pattern described above. The magnitude and sign of $\Delta\Gamma$ and of the Δb_i values for each of the $[\text{M}(\text{CO})_5\{\text{P}(\text{OCH}_2)_3\text{CMe}\}]$ complexes provide direct and convincing evidence for substantial π character for the P-M bonds in these complexes and for conjugative delocalisation along the P-M-CO(*trans*) axis.

X-Ray Crystal Structure Analysis.—The complex $[\text{Mo}(\text{CO})_5-$

Table 4 Positional parameters ($\times 10^4$) for $[\text{Mo}(\text{CO})_5\{\text{P}(\text{OCH}_2)_3\text{CMe}\}]$

Atom	x	y	z
Mo(1)	1909(1)	7243(1)	3472(1)
P(1)	3944(1)	7236(1)	2810(1)
O(1)	5091(3)	7874(4)	3586(3)
O(2)	4016(3)	7925(3)	1694(3)
O(3)	4530(4)	5906(3)	2603(4)
C(1)	6335(5)	7821(7)	3215(5)
C(2)	5252(5)	7971(7)	1326(4)
C(3)	5731(6)	5933(6)	2173(6)
C(4)	6227(5)	7227(5)	2095(4)
C(5)	7510(6)	7236(7)	1689(5)
C(6)	1249(6)	5935(7)	2343(6)
O(4)	882(6)	5263(6)	1673(6)
C(7)	2572(6)	5862(7)	4500(6)
O(5)	2947(5)	5057(5)	5048(4)
C(8)	2590(6)	8607(6)	4542(5)
O(6)	2967(5)	9390(5)	5095(4)
C(9)	1266(6)	8573(7)	2351(6)
O(7)	933(5)	9282(6)	1714(5)
C(10)	262(6)	7254(7)	4120(5)
O(8)	-640(4)	7260(6)	4514(5)

$\{\text{P}(\text{OCH}_2)_3\text{CMe}\}$ crystallises with no close contacts between the neutral complex molecules. A view of the molecule with atom labelling is given in Fig. 2, atomic coordinates are given in Table 4 and bond lengths and angles in Table 5. The molybdenum atom is octahedrally co-ordinated with average angles between the *cis* CO ligands $C_{\text{cis}}-\text{M}-C_{\text{cis}}$ of 90.0° . The molybdenum-phosphorus bond length found for this compound is considerably shorter than the P-M bond lengths reported for $[\text{Mo}(\text{CO})_5\{\text{P}(\text{CH}_2\text{CH}_2\text{CN})_3\}]$ and $[\text{Mo}(\text{CO})_5(\text{PPh}_3)]$ by Cotton *et al.*⁴¹ from X-ray crystal structure analyses, but longer than that reported by Bridges *et al.*⁴² for $[\text{Mo}(\text{CO})_5(\text{PF}_3)]$, examined by gas-phase electron diffraction (see Table 6). The shorter P-M bond is consistent with more pronounced π character for this bond in $[\text{Mo}(\text{CO})_5\{\text{P}(\text{OCH}_2)_3\text{CMe}\}]$ relative to the complexes studied by Cotton *et al.*⁴¹ though the effect of steric repulsions between the different phosphorus ligands and equatorial CO groups cannot be discounted. On the basis of the P-Mo bond lengths shown in Table 6, $\text{P}(\text{OCH}_2)_3\text{CMe}$ appears to have π -acceptor capability intermediate between the very strong π -accepting PF_3 and the trialkyl- or triaryl-phosphines.

Further information on interligand interactions comes from comparison of M-C bond lengths *cis*- and *trans*- to phosphorus. It is seen that M-C_{*trans*} is sensitive to changes in phosphine ligand, decreasing in the order $\text{PF}_3 > \text{P}(\text{OCH}_2)_3\text{CMe} > \text{P}(\text{CH}_2\text{CH}_2\text{CN})_3 > \text{PPh}_3$. By contrast, M-C_{*cis*} is almost invariant ($2.044 \pm 0.002 \text{ \AA}$) except for $[\text{Mo}(\text{CO})_5(\text{PF}_3)]$ which is somewhat larger (2.063 \AA). The sequence of decreasing M-C_{*trans*} bond distances correlates with that of increasing P-M bond lengths as predicted by π -bonding arguments.² The carbonyl bond lengths show no obvious trend; they are not acutely affected by changes in the CO bond order in these complexes.⁴³

Table 5 Bond lengths (Å) and angles (°) for [Mo(CO)₅{P(OCH₂)₃CMe}]

P–Mo	2.417(1)	O(1)–P	1.601(4)	C(3)–O(3)	1.451(6)	O(4)–C(6)	1.133(8)
C(6)–Mo	2.046(8)	O(2)–P	1.589(4)	C(4)–C(1)	1.524(8)	O(5)–C(7)	1.142(8)
C(7)–Mo	2.025(7)	O(3)–P	1.600(4)	C(4)–C(2)	1.535(7)	O(6)–C(8)	1.128(7)
C(8)–Mo	2.048(7)	C(1)–O(1)	1.460(6)	C(4)–C(3)	1.500(8)	O(7)–C(9)	1.124(8)
C(9)–Mo	2.052(8)	C(2)–O(2)	1.450(6)	C(5)–C(4)	1.518(8)	O(8)–C(10)	1.137(7)
C(10)–Mo	2.026(6)						
C(6)–Mo–P	90.0(2)	C(7)–Mo–P	88.0(2)	O(3)–P–O(2)	102.2(2)	C(1)–O(1)–P	115.9(3)
C(7)–Mo–C(6)	89.0(3)	C(8)–Mo–P	88.5(2)	C(2)–O(2)–P	116.7(3)	C(3)–O(3)–P	115.0(3)
C(8)–Mo–C(6)	117.2(3)	C(8)–Mo–C(7)	93.2(2)	C(4)–C(1)–O(1)	110.5(5)	C(4)–C(2)–O(2)	110.2(4)
C(9)–Mo–P	89.9(2)	C(9)–Mo–C(6)	88.0(3)	C(4)–C(3)–O(3)	112.2(5)	C(2)–C(4)–C(1)	108.1(5)
C(9)–Mo–C(7)	176.4(3)	C(9)–Mo–C(8)	89.7(2)	C(3)–C(4)–C(1)	108.3(5)	C(3)–C(4)–C(2)	108.3(5)
C(10)–Mo–P	176.5(2)	C(10)–Mo–C(6)	92.6(3)	C(5)–C(4)–C(1)	110.3(5)	C(5)–C(4)–C(2)	110.3(5)
C(10)–Mo–C(7)	89.8(3)	C(10)–Mo–C(8)	89.0(3)	C(5)–C(4)–C(3)	111.5(5)	O(4)–C(6)–Mo	176.0(7)
C(10)–Mo–C(9)	92.5(3)	O(1)–P–Mo	115.7(1)	O(5)–C(7)–Mo	177.5(6)	O(6)–C(8)–Mo	177.0(6)
O(2)–P–Mo	116.9(2)	O(2)–P–O(1)	101.7(2)	O(7)–C(9)–Mo	177.8(6)	O(8)–C(10)–Mo	177.9(6)
O(3)–P–Mo	116.4(1)	O(3)–P–O(1)	101.7(2)				

Table 6 Comparison of structural parameters of [M(CO)₅L] complexes

Ligand L	P(OCH ₂) ₃ CMe	P(CH ₂ CH ₂ CN) ₃ ^a	PPh ₃ ^a	PF ₃ ^b
M–P	2.417	2.506	2.560	2.37
M–C _{trans}	2.026	2.008	1.995	2.063
M–C _{cis}	2.043	2.044	2.046	2.063
C–O _{trans}	1.137	1.145	1.142	1.154
C–O _{cis}	1.132	1.133	1.134	1.154
C _{trans} –M–C _{cis}	91.0	89.9	88.6	88 ± 2
P–M–C _{cis}	89.1	90.2	91.5	—
C _{trans} –M–P	176.5	177.4	174.4	—
C _{cis} –M–C _{cis}	90.0	90.3	90.0	—

^a Data from ref. 41. ^b Data from ref. 42.

Bond parameters for co-ordinated P(OCH₂)₃CMe are compared with analogous distances for OP(OCH₂)₃CMe and [Ag{P(OCH₂)₃CMe}₄]⁺ reported by Verkade.²¹ The ring P–O bond length in OP(OCH₂)₃CMe is 1.57 Å which is shorter than that found in [Mo(CO)₅{P(OCH₂)₃CMe}] (1.597 Å); the P–O–C angle is virtually the same in both the oxide and the molybdenum carbonyl complex. The O–P–O angle now found (101.9°) is a little larger than for [Ag{P(OCH₂)₃CMe}₄]⁺ (99°).²¹

The four equatorial CO groups in [Mo(CO)₅{P(OCH₂)₃CMe}] are inclined slightly (1°) towards the P(OCH₂)₃CMe ligand. Small deviations of 0.2 and 1.5° away from the phosphorus ligand are observed for [Mo(CO)₅{P(CH₂CH₂CN)₃}] and [Mo(CO)₅(PPh₃)], respectively.⁴¹ The equatorial CO groups in [Mo(CO)₅(PF₃)] were found by Bridges *et al.*⁴² to be bent away from PF₃ (2 ± 2°), and they stated 'equatorial carbonyl groups are usually bent (at the metal) away from the stronger π-acceptor axial ligand, and so trifluorophosphine would appear to be marginally better as an acceptor than a carbonyl group.'

In all of the complexes the phosphorus ligand is displaced by several degrees relative to M–CO_{trans}. In the case of [Cr(CO)₅(PMe₃)], Lee and Brown¹⁶ attribute this distortion to a symmetry mismatch between PMe₃ (three-fold symmetry) and the Cr(CO)₄ plane (four-fold symmetry). Another contributing factor could be intermolecular interactions in the crystal lattice. Cotton *et al.*⁴¹ have suggested that the tilting may help alleviate steric interactions between the phosphorus ligand and the equatorial carbonyl groups. The small variation in P–M–CO_{eq} angles indicates repulsion is not a major factor in these complexes.

Conclusion

Electric dipole moments, polarisability tensors, carbonyl infrared vibrations and interatomic distances of complexes

[M(CO)₅{P(OCH₂)₃CMe}] where M = Cr, Mo or W, have been examined to obtain information on phosphorus–metal interactions. The combined results provide strong evidence for an important π component in the P–M bonding for these compounds. Analysis of the molecular optical anisotropies and directional polarisabilities shows pronounced enhancement of polarisability specifically along the P–M–CO(*trans*) axis with concomitant diminution perpendicular to that axis, demonstrating the inadequacy of a hypothetical reference model with a purely σ-bonded P–M. Comparisons are made with other [M(CO)₅L] systems where L is qncd, PMe₃ or PCl₃. The structural data for [Mo(CO)₅{P(OCH₂)₃CMe}] reported herein, further support significant π character in the P–M bond.

Acknowledgements

The authors acknowledge with gratitude assistance by Dr. L. Phillips with computing and the granting to M. S. D. of an Australian Postgraduate Research Award.

References

- F. A. Cotton and G. Wilkinson, *Advanced Inorganic Chemistry*, Wiley-Interscience, New York, 5th edn., 1988, pp. 65–68.
- J. E. Huheey, *Inorganic Chemistry*, Harper and Row, New York, 3rd edn., 1983, pp. 432–441.
- R. H. Crabtree, *The Organometallic Chemistry of the Transition Metals*, Wiley, New York, 1988, pp. 71–74.
- P. Powell, *Principles of Organometallic Chemistry*, Chapman and Hall, London, 2nd edn., 1988, pp. 160–161.
- M. M. Rahman, H. Y. Liu, A. Prock and W. P. Giering, *Organometallics*, 1987, **6**, 650.
- H. Y. Liu, K. Eriks, A. Prock and W. P. Giering, *Organometallics*, 1990, **9**, 1758.
- M. M. Rahman, H. Y. Liu, K. Eriks, A. Prock and W. P. Giering, *Organometallics*, 1989, **8**, 1.
- M. N. Golovin, M. M. Rahman, J. E. Belmonte and W. P. Giering, *Organometallics*, 1985, **4**, 1981.

- 9 G. Pacchioni and P. S. Bagus, *Inorg. Chem.*, 1992, **31**, 4391.
- 10 S. X. Xiao, W. C. Trogler, D. E. Ellis and Z. Berkovitch-Yellin, *J. Am. Chem. Soc.*, 1983, **105**, 7033.
- 11 D. S. Marynick, *J. Am. Chem. Soc.*, 1984, **106**, 4064.
- 12 M. J. Aroney, M. K. Cooper, R. K. Pierens and S. J. Pratten, *J. Organomet. Chem.*, 1986, **309**, 293.
- 13 M. J. Aroney, R. M. Clarkson, T. W. Hambley and R. K. Pierens, *J. Organomet. Chem.*, 1992, **426**, 331.
- 14 M. S. Davies, R. K. Pierens and M. J. Aroney, *J. Organomet. Chem.*, 1993, **458**, 141.
- 15 M. L. Caffery and T. L. Brown, *Inorg. Chem.*, 1991, **30**, 3907.
- 16 K. J. Lee and T. L. Brown, *Inorg. Chem.*, 1992, **31**, 289.
- 17 T. L. Brown, *Inorg. Chem.*, 1992, **31**, 1286.
- 18 C. W. Heitsch and J. G. Verkade, *Inorg. Chem.*, 1962, **1**, 392.
- 19 J. G. Verkade, T. J. Guttemann, M. K. Fung and R. W. King, *Inorg. Chem.*, 1965, **4**, 85.
- 20 J. G. Verkade, R. E. McCarley, D. G. Hendricker and R. W. King, *Inorg. Chem.*, 1965, **4**, 228.
- 21 J. G. Verkade, *Coord. Chem. Rev.*, 1972/73, **9**, 1.
- 22 C. G. Le Fèvre and R. J. W. Le Fèvre, in *Techniques of Chemistry*, ed. A. Weissberger, Wiley-Interscience, New York, 1972, vol. 1, Part III C.
- 23 R. J. W. Le Fèvre, *Dipole Moments*, Methuen, London, 1953.
- 24 Enraf-Nonius Structure Determination Package, Enraf Nonius, Delft, Holland, 1985.
- 25 G. M. Sheldrick, SHELX 76, A Program for X-Ray Crystal Structure Determination, University of Cambridge, 1976.
- 26 *International Tables for X-Ray Crystallography*, Kynoch Press, Birmingham, 1974, vol. 4.
- 27 C. K. Johnson, ORTEP, A Thermal Ellipsoid Plotting Program, Oak Ridge National Laboratories, Oak Ridge, TN, 1965.
- 28 R. E. Dessy and L. Wiczorek, *J. Am. Chem. Soc.*, 1969, **91**, 4963.
- 29 G. Keeling, S. F. A. Kettle and I. Paul, *J. Chem. Soc. A*, 1971, 3143.
- 30 M. J. Aroney, R. J. W. Le Fèvre and J. D. Saxby, *J. Chem. Soc.*, 1963, 4938.
- 31 P. Cassoux, R. L. Kuczkowski, P. S. Bryan and R. C. Taylor, *Inorg. Chem.*, 1975, **14**, 126.
- 32 P. S. Bryan and R. L. Kuczkowski, *Inorg. Chem.*, 1972, **11**, 553.
- 33 R. S. Armstrong, M. J. Aroney, R. J. W. Le Fèvre, R. K. Pierens, J. D. Saxby and C. J. Wilkins, *J. Chem. Soc. A*, 1969, 2735.
- 34 R. J. W. Le Fèvre, *Adv. Phys. Org. Chem.*, 1965, **3**, 1.
- 35 M. J. Aroney, M. K. Cooper, R. K. Pierens, S. J. Pratten and S. W. Filipczuk, *J. Organomet. Chem.*, 1985, **295**, 333.
- 36 R. S. Armstrong, M. J. Aroney, K. E. Calderbank and R. K. Pierens, *Aust. J. Chem.*, 1977, **30**, 1411.
- 37 R. S. Armstrong, G. J. Peacock, K. R. Skamp and R. J. W. Le Fèvre, *J. Chem. Soc., Dalton Trans.*, 1973, 1132.
- 38 R. Bramley and R. J. W. Le Fèvre, *J. Chem. Soc.*, 1960, 1820.
- 39 M. J. Aroney, K. E. Calderbank, R. J. W. Le Fèvre and R. K. Pierens, *J. Chem. Soc. B*, 1969, 159; 1970, 1120.
- 40 U. W. Suter and P. J. Flory, *J. Chem. Soc., Faraday Trans. 2*, 1977, **73**, 1521.
- 41 F. A. Cotton, D. J. Darensbourg and W. H. Ilsley, *Inorg. Chem.*, 1981, **20**, 578.
- 42 D. M. Bridges, G. C. Holywell, D. W. H. Rankin and J. M. Freeman, *J. Organomet. Chem.*, 1971, **32**, 87.
- 43 F. A. Cotton and R. M. Wing, *Inorg. Chem.*, 1965, **4**, 314.

Received 22nd July 1993; Paper 3/04300B